https://doi.org/10.15407/ujpe70.7.477

M.YA. RUDYSH,[1] M. PIASECKI,[2] A.I. KASHUBA,[3] R.S. BREZVIN[1]

[1] Ivan Franko National University of Lviv
*(8, Kyryla i Mefodiya Str., Lviv 79005, Ukraine; e-mail: rudysh.myron@gmail.com)*
[2] Uniwersytet Jana Długosza w Częstochowie
*(Al. Armii Krajowej, 13/15, Częstochowa 42-200, Polska)*
[3] National University "Lviv Polytechnic"
*(12, Stepana Bandery Str., Lviv 79013, Ukraine)*

# VIBRATIONAL SPECTRA OF THE $(NH_4)_2BeF_4$ CRYSTAL IN THE PARAELECTRIC PHASE

*The vibrational spectra of the $(NH_4)_2BeF_4$ crystal in the paraelectric phase (the space group symmetry No. 62) have been studied. In the framework of the group-theoretical analysis, the symmetry of vibrations in the crystal is classified. Using the first-principles approach and in the framework of the density functional theory and the density perturbation functional theory, the dispersion of phonons and the frequencies of the vibrational spectrum of the $(NH_4)_2BeF_4$ crystal are calculated. To describe the exchange-correlation interaction of electrons, the generalized gradient approximation is applied. 180 vibrational modes are found in the vibrational spectrum of the examined crystal. The infrared and Raman spectra of the $(NH_4)_2BeF_4$ crystal are calculated and compared with experimental ones.*

*K e y w o r d s*: phonon, ammonium fluoroberylate, DFPT, group theory, infrared spectra, Raman spectra, phonon density of states.

## 1. Introduction

Crystals of ammonium fluoroberylate $(NH_4)_2BeF_4$ (FBA) are a dielectric material isomorphic to ammonium sulfate ($(NH_4)_2SO_4$). They are an interesting research object due to the presence of atoms of light chemical elements, such as hydrogen and beryllium, in the FBA composition. Furthermore, fluorine atoms have the highest electronegativity among all other chemical elements, which can be reflected in the properties of materials that contain them.

$(NH_4)_2BeF_4$ crystals are grown from an aqueous solution by either evaporating the solvent [1] or lowering the temperature [2]. The starting material is the salt $(NH_4)_2BeF_4$, which is dissolved in demineralized water. It is known that the crystals are transparent and colorless. At room temperature, $(NH_4)_2BeF_4$ crystals have the space group symmetry *Pnma* (group No. 62) with the lattice parameters $a = 7.531$ Å, $b = 5.874$ Å, $c = 10.399$ Å, $V = 460.02$ Å$^3$, and $Z = 4$ [3]. This crystal phase is paraelectric [4]. As the temperature decreases, two phase transitions occur: at the temperatures $T = 182$ and 175 K [3, 5] (Fig. 1). Between them, the crystal is in a phase with an incommensurately modulated structure with the modulation vector $\mathbf{q} = 0.5\,\mathbf{a}^*$ [6]. At the temperature $T = 175$ K, a cell-doubling ($a = 2a_0$) phase transition takes place with the transformation of the crystal structure into a structure with the space group

Citation: Rudysh M.Ya., Piasecki M., Kashuba A.I., Brezvin R.S. Vibration spectra of the $(NH_4)_2BeF_4$ crystal in paraelectric phase. *Ukr. J. Phys.* **70**, No. 7, 477 (2025). https://doi.org/10.15407/ujpe70.7.477.


***Fig. 1.*** Schematic diagram of the temperature distribution of the phases and phase transitions of the $(NH_4)_2BeF_4$ crystal

symmetry $Pcn2_1$ and the parameters $a = 14.997$ Å, $b = 5.860$ Å, $c = 10.402$ Å, and $V = 914.1$ Å$^3$ [3]. This low-temperature phase is ferroelectric.

The study of Raman spectra is an effective method for analyzing the dynamics of the crystal lattice and the molecules of substances. Together with infrared spectra, such studies make it possible to study and analyze optical vibrations of the structural elements of crystals. These two methods are complementary, and together they provide information about various types of vibrations in the material. Earlier, the infrared spectra of the $(NH_4)_2BeF_4$ crystal were studied in a wide spectral interval in work [1]. M. Wada *et al.* performed temperature studies of the Raman spectra in the frequency interval from 0 to 200 cm$^{-1}$ [7].

A small number of experimental studies carried out in a narrow spectral frequency interval and with a low resolution do not allow the vibrational spectrum of the crystal to be analyzed in detail. At the same time, theoretical calculations of the vibrational spectrum of the $(NH_4)_2BeF_4$ crystal have not been done yet.

In this work, a theoretical study of the vibrational spectrum of the $(NH_4)_2BeF_4$ crystal in the paraelectric phase has been carried out. Using the group-theoretical analysis, a symmetry classification of phonon modes is made. In the framework of the density functional theory (DFT) and the density functional perturbation theory (DFPT), the vibrational spectrum of the $(NH_4)_2BeF_4$ crystal is calculated. The infrared and Raman spectra are also obtained using the generalized gradient approximation (GGA).

## 2. Technique of Vibrational Spectrum Calculation

The vibrational spectra of the $(NH_4)_2BeF_4$ crystals are calculated using the CASTEP program [8, 9], which is a software implementation of the density functional theory [10]. As initial calculation parameters were chosen the crystallographic data obtained for the $(NH_4)_2BeF_4$ crystal in work [3]. The system energy was obtained from the self-consistent solution of the Kohn–Sham equations [11]. The wave functions of the valence electrons were described by flat Bloch-type functions [12]. The electronic configuration of the valence electrons was taken as follows: H $1s^1$, Be $2s^2$, N $2s^2\ 2p^3$, and F $2s^2\ 2p^5$. The plane-wave cutoff energy was $E_{\text{cut}} = 850$ eV.

The norm-conserving pseudopotential method was applied to describe the core electrons [13]. The exchange-correlation interaction was described using the generalized gradient approximation (GGA) with the Perdew–Burke–Ernzerhof (PBE) parameterization. The integration was performed on a $4 \times 5 \times 4$ $k$-grid, which was selected using the Monkhorst–Pack method [14]. The phonon spectrum was calculated by applying the finite displacement method in the framework of the density functional perturbation theory [15].

When constructing the phonon dispersion $\omega(q)$ in the studied material, frequency calculations were performed for various $q$-points in the first Brillouin zone. Before calculating the phonon spectrum, the crystal lattice structure was optimized. For this purpose, the Broyden–Fletcher–Goldfarb–Shanno (BFGS) algorithm was applied to the experimental lattice [16]. The convergence criteria for the optimization were as follows: the convergence of the self-consistent field was $10^{-6}$ eV/atom, the energy was $5 \times 10^{-6}$ eV/atom, the maximum force was $1 \times 10^{-2}$ eV/A, the maximum pressure was $2 \times 10^{-2}$ GPa, and the maximum displacement of atoms was $5 \times 10^{-4}$ Å.

## 3. Results and Discussion

### *3.1. Structure of $(NH_4)_2BeF_4$ crystals*

The crystallographic parameters of the $(NH_4)_2BeF_4$ crystal were used as initial data for calculating the vibrational spectra. Information about the structure of the studied material was taken from work [3], where

X-ray studies were performed. The crystal lattice parameters and the relative atomic coordinates are quoted in Tables 1 and 2, respectively.

In Fig. 2, the schematic diagram of the crystal lattice of $(NH_4)_2BeF_4$ is shown. Here, the blue, white, green, and red balls correspond to nitrogen, hydrogen, beryllium, and fluorine atoms, respectively. The figure demonstrates that the atoms in the cell form tetrahedral complexes of two types; namely, the cationic group $[NH_4]^+$ and the anionic group $[BeF_4]^{2-}$. Both complexes consist of chemical elements of two types, which have a relatively small mass. The presence of such isolated complexes suggests that these specific features of the material may manifest themselves in its properties, in particular, in the electronic structure and the vibrational spectra.

*Table 1.* **Experimental values of the lattice parameters of the crystal $(NH_4)_2BeF_4$ in the paraelectric phase and the corresponding theoretical values optimized using the GGA-PBE functional**

| Parameter | Experiment [3] | Calculations |
|---|---|---|
| Space group No. | 62 | 62 |
| $a$, Å | 7.531 | 7.587 |
| $b$, Å | 5.874 | 6.830 |
| $c$, Å | 10.399 | 10.941 |
| $V$, Å$^3$ | 460.02 | 566.95 |
| $Z$ | 4 | 4 |

*Table 2.* **Relative coordinates of atoms in the crystal lattice of $(NH_4)_2BeF_4$ salt taken from work [3] and obtained using the GGA-PBE functional**

| Atom | Calculations (GGA-PBE) | | | Experiment [3] | | |
|---|---|---|---|---|---|---|
| | $x/a$ | $y/b$ | $z/c$ | $x/a$ | $y/b$ | $z/c$ |
| N1 | 0.1850 | 0.2500 | 0.09900 | 0.1804(6) | 0.25 | 0.0968(4) |
| N2 | 0.4610 | 0.2500 | 0.80440 | 0.4687(6) | 0.25 | 0.8059(4) |
| Be | 0.2505 | 0.2500 | 0.41840 | 0.2466(7) | 0.25 | 0.4180(5) |
| F1 | 0.0531 | 0.2500 | 0.38170 | 0.0502(4) | 0.25 | 0.3933(3) |
| F2 | 0.2747 | 0.2500 | 0.56390 | 0.2856(4) | 0.25 | 0.5620(3) |
| F3 | 0.3354 | 0.0348 | 0.36380 | 0.3278(3) | 0.0365(3) | 0.3588(2) |
| H1 | 0.3137 | 0.2500 | 0.12440 | 0.288(7) | 0.25 | 0.108(4) |
| H2 | 0.0996 | 0.2500 | 0.17110 | 0.109(7) | 0.25 | 0.156(5) |
| H3 | 0.1639 | 0.1137 | 0.04970 | 0.167(4) | 0.115(5) | 0.048(3) |
| H4 | 0.4897 | 0.2500 | 0.71060 | 0.491(7) | 0.25 | 0.739(5) |
| H5 | 0.5686 | 0.2500 | 0.85960 | 0.547(7) | 0.25 | 0.856(5) |
| H6 | 0.3854 | 0.1174 | 0.82380 | 0.392(4) | 0.115(5) | 0.823(3) |

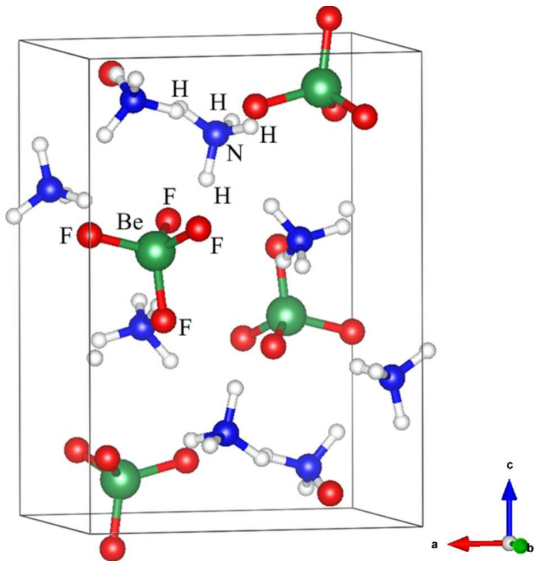


***Fig. 2.*** Crystal lattice of the $(NH_4)_2BeF_4$ crystal obtained using the VESTA program [17]

Before calculating the vibrational properties, a mandatory geometric optimization of the structure was carried out. This stage is important for obtaining a well-relaxed crystal structure and, as a consequence, correct results. In this work, a full geometric optimization was performed, which included the search for equilibrium lattice parameters and atomic coordinates that corresponded to the ground state of the system. During the optimization procedure, the symmetry of the unit cell was fixed. The crystal lattice parameters of the ammonium fluoroberyllate crystal, which were obtained using the geometric optimization method, are given in Table 1, and, for comparison, experimental data of X-ray analysis taken from the literature are also quoted [3].

As one can see from Table 1, the functional parameters of the crystal lattice optimized using the GGA-PBE method are close to the experimental ones. For the optimized structure, the lattice parameters are overestimated, and, as a result, an increase in the unit cell volume is observed. Such an overestimation was observed earlier for some other crystals [18–20], and it can be attributed to the general characteristic of optimization based on the GGA-PBE method. The lattice parameter $a$ of the $(NH_4)_2BeF_4$ crystal almost

coincides with the experimental data (the deviation is less than 1%). The parameters $b$ and $c$ demonstrate larger deviations equal to 16% and 5%, respectively. The volume of the optimized crystal lattice is larger by 23% than the experimentally obtained value.

### *3.2. Symmetry classification of the vibrational modes of the $(NH_4)_2BeF_4$ crystal*

In practice, the most interesting to study are the first-order phonon spectra, when excited are the vibrational modes of the crystal that are close to the center of the Brillouin zone (point Γ). In such studies, the magnitude of the light wave vector is substantially smaller than the size of the first Brillouin zone of the crystal. As a result, in most cases, the analysis of phonon spectra is concentrated at the center of the Brillouin zone ($\mathbf{k} = 0$).

The symmetry classification of vibrational modes of molecules and crystalline materials makes it possible to find out possible types of vibrations in the structure, find their number, symmetry, and degeneracy, and, according to the selection rules, determine allowed transitions. The classification of vibrational spectra is carried out using the group theory methods described in work [21]. The general method of vibrational classification uses the theory of characters of irreducible representations; it is based on finding the complete vibrational representation and its subsequent expansion into irreducible representations of the crystal factor group. The character of the complete vibrational representation $\chi(R)$ is defined as follows:

$$\chi(R) = n_0(R)(\pm 1 + 2\cos\theta_R), \tag{1}$$

where $R$ is the symmetry element of the crystal factor group, $n_0(R)$ is the number of atoms that remain in place after the symmetry operation $R$ with an accuracy of the primitive translation vector, and $\theta_R$ is the rotation angle under the symmetry operation $R$. The sign in the expression is chosen to be positive for proper rotations and negative for improper ones.

The character of the complete representation $\chi(R)$ contains the characters of both acoustic and optical vibrations,

$$\chi_a(R) = \pm 1 + 2\cos\theta_R, \tag{2}$$

$$\chi_{\text{opt.}}(R) = (n_0(R) - 1)(\pm 1 + 2\cos\theta_R). \tag{3}$$

Using the reduction formula, the representation character of optical vibrations can be expanded into irreducible representations of the crystal point group $G_0$ as follows:

$$m_i = \frac{1}{h}\sum_R N_j \chi_{\text{opt.}}(R_j)[\chi^i(R_j)], \tag{4}$$

where $m_i$ is a number showing how many times the $i$-th irreducible representation of the group $G_0$ is contained in the vibrational representation $\chi_{\text{opt.}}(R)$, $h$ is the order of the group $G_0$, $\chi^i(R_j)$ is the character of the $j$-th irreducible representation for the operation $R_j$, and $N_j$ is the number of operations of the $j$-th class.

As was mentioned above, the crystal lattice $(NH_4)_2BeF_4$ belongs to the orthorhombic system with the space group symmetry $Pnma$ (No. 62). It is isomorphic to the point symmetry group $D_{2h}$. The order of this group equals $h = 8$. For the crystal lattice of $(NH_4)_2BeF_4$ in the paraelectric phase, the following symmetry operators are available:

$\{(x, y, z)|(0, 0, 0)\}$;
$\{(-x, -y, -z)|(0.5, 0, 0.5)\}$;
$\{(-x, y, -z)|(0, 0.5, 0)\}$;
$\{(x, -y, -z)|(0.5, 0.5, 0.5)\}$;
$\{(-x, -y, -z)|(0, 0, 0)\}$;
$\{(x, y, -z)|(0.5, 0, 0.5)\}$;
$\{(x, -y, z)|(0, 0.5, 0)\}$;
$\{(-x, y, z)|(0.5, 0.5, 0.5)\}$.

A unit cell of the $(NH_4)_2BeF_4$ crystal contains $Z = 4$ formula units, so the number of atoms contained in it equals $N = 15Z = 15 \times 4 = 60$, where $N$ is the number of atoms in the formula unit. While performing the symmetry analysis of $(NH_4)_2BeF_4$, the entire lattice was taken into account, because this structure does not contain a primitive lattice. Therefore, in order to describe vibrations, it is necessary to take $N = 60$ atoms into account, which ultimately gives $3N = 180$ different normal modes in the phonon spectrum of the crystal.

Table 3 demonstrates the characters of the point symmetry group $D_{2h}$. The elements of this group are as follows: $E$ is the identity operator, $C_2(x)$ is the second-order symmetry axis directed along the $x$-axis, $C_2(y)$ is the second-order symmetry axis directed

*Table 3.* **Characters of irreducible representations for the point group $D_{2h}$**

| $D_{2h}$ | $E$ | $C_2(z)$ | $C_2(y)$ | $C_2(x)$ | $i$ | $\sigma(xy)$ | $\sigma(xz)$ | $\sigma(yz)$ | Linear functions | Quadratic functions |
|---|---|---|---|---|---|---|---|---|---|---|
| $B_{2u}$ | 1 | –1 | 1 | –1 | –1 | 1 | –1 | 1 | $y$ | |
| $B_{1u}$ | 1 | 1 | –1 | –1 | –1 | –1 | 1 | 1 | $z$ | |
| $B_{3u}$ | 1 | –1 | –1 | 1 | –1 | 1 | 1 | –1 | $x$ | |
| $A_g$ | 1 | 1 | 1 | 1 | 1 | 1 | 1 | 1 | | $x^2$, $y^2$, $z^2$ |
| $B_{3g}$ | 1 | –1 | –1 | 1 | 1 | –1 | –1 | 1 | $R_x$ | $yx$ |
| $A_u$ | 1 | 1 | 1 | 1 | –1 | –1 | –1 | –1 | | |
| $B_{1g}$ | 1 | 1 | –1 | –1 | 1 | 1 | –1 | –1 | $R_x$ | $xy$ |
| $B_{2g}$ | 1 | –1 | 1 | –1 | 1 | –1 | 1 | –1 | $R_y$ | $xz$ |

along the $y$-axis, $C_2(z)$ is the second-order symmetry axis directed along the $z$-axis, $i$ is the inversion operator, $\sigma(xy)$ is the plane of symmetry reflecting in the $xy$-plane; $\sigma(xz)$ is the plane of symmetry reflecting in the $xz$-plane, and $\sigma(yz)$ is the plane of symmetry reflecting in the $yz$-plane.

Using the standard method [21], the group-theoretical analysis of the vibrational spectrum was carried out, and the following irreducible representation of the total vibrational spectrum was obtained:

$$\Gamma = 27A_g + 18B_{1g} + 27B_{2g} + 18B_{3g} + \\ + 18A_u + 27B_{1u} + 18B_{2u} + 27B_{3u}. \quad (5)$$

By expanding the complete vibrational representation (6), the characters of the vibrational representations $\Gamma_v$ and acoustic vibrations $\Gamma_a$ were calculated. As a result, the following classification was obtained:

$$\Gamma_v = 27A_g + 18B_{1g} + 27B_{2g} + 18B_{3g} + \\ + 18A_u + 26B_{1u} + 17B_{2u} + 26B_{3u}, \quad (6)$$

$$\Gamma_a = B_{1u} + B_{2u} + B_{3u}. \quad (7)$$

The modes $B_{1u}$, $B_{2u}$, and $B_{3u}$ form acoustic branches and correspond to the translations $T_x$, $T_y$, and $T_z$ along the main crystallographic axes $x$, $y$, and $z$ (external modes). The modes $A_g$ are completely symmetric vibrations; and the modes $B_{1u}$, $B_{2u}$, and $B_{3u}$ are external translations. The vibrational modes of the $B_{1g}$ and $B_{3g}$ symmetries are close to librational.

Using the group-theoretical analysis, it is possible to obtain information about the structures of infrared and Raman spectra. The fundamental vibrations observed in infrared spectra can be obtained by analyzing the symmetry of the dipole moment components $\mu$. This classification takes into account active vibrations during which the dipole moment component changes. In order for the representation $\Gamma_i$ to be active in infrared spectra, the following condition must hold:

$$\frac{1}{h}\sum_R(\pm 1 + 2\cos\theta_R)a_a(R) \neq 0, \quad (8)$$

where $h$ is the group order, $\theta_R$ is the rotation angle after the symmetry operation $R$ is done, and $a_a$ are the coefficients of the expansion in the characters of the irreducible representations for acoustic modes.

The components of the dipole moment of the $(NH_4)_2BeF_4$ crystal have the symmetries $B_{1u}$, $B_{2u}$, and $B_{3u}$. Given this, the infrared spectrum contains the following vibrations:

$$\Gamma_\alpha = 26B_{1u} + 17B_{2u} + 26B_{3u}. \quad (9)$$

Whence it follows that the infrared spectra contain 69 vibrational modes corresponding to the fundamental vibrations in the crystal lattice.

For Raman scattering spectra, the condition for the activity of the $(NH_4)_2BeF_4$ crystal lattice vibration is the consistency of the representation $\Gamma_i$ with the representation obtained by the components of the symmetric tensor:

$$\frac{1}{h}\sum_R[2\cos\theta_R(\pm 1 + 2\cos\theta_R)]a_i(R) \neq 0. \quad (10)$$

Thus, for the $(NH_4)_2BeF_4$ crystal, the Raman spectra are represented by the $A_g$, $B_{1g}$, $B_{2g}$, and $B_{3g}$ active modes, which together include the fundamental oscillations

$$\Gamma_v = 27A_g + 18B_{1g} + 27B_{2g} + 18B_{3g}. \quad (11)$$

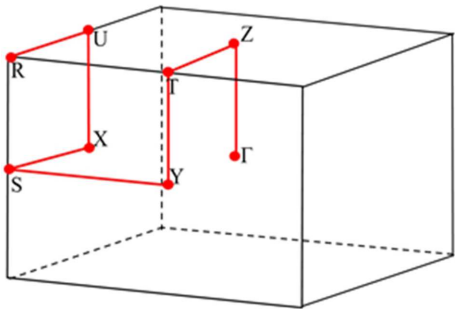


***Fig. 3.*** First Brillouin zone of the $(NH_4)_2BeF_4$ crystal

It is worth noting that the vibrational modes of the $A_u$ symmetry are inactive in the vibrational spectrum.

### *3.3. Phonon spectrum of the $(NH_4)_2BeF_4$ crystal*

The dispersion of phonons in the $(NH_4)_2BeF_4$ crystal was calculated at the high-symmetry points in the first Brillouin zone and along the lines connecting them in the following sequence: $\Gamma \to Z \to T \to \to Y \to S \to X \to U \to R$. The structure of the first Brillouin zone is shown in Fig. 3. To calculate the phonon spectrum, the optimized structural parameters of the crystal given in Tables 1 and 2 were taken as the initial data.

When calculating the phonon spectrum of crystalline materials, it is important to use a well-optimized crystal structure. As a result, high-quality results can be obtained, which often agree well with experimental data. Earlier [22, 23], the phonon spectrum in the $LiNH_4SO_4$ crystal was studied using first-principles calculations and in the framework of the methodology applied in this work, and the results obtained were in good agreement with the experiment.

In Fig. 4, *a*, the phonon dispersion in the $(NH_4)_2BeF_4$ crystal calculated by integrating over the first Brillouin zone (Fig. 3) is shown. The phonon dispersion comprises a set of narrow bands corresponding to optical branches of phonons. From the phonon density of states, it is clear that the vibrational bands have similar intensities (Fig. 4, *b*). The optical branches have weak dispersion. This can be a result of the previously mentioned isolation of the structural complexes. The phonon dispersion contains 180 vibrational spectral modes, which is consistent with the group-theoretical analysis of the crystal structure. The maximum vibrational frequency in the spectrum is 3202 $cm^{-1}$. The high frequency of the vibrational branches follows from the availability of light ions in the crystal structure, which vibrate at high frequencies $v \sim 1/m$ (in particular, $m_F = 18.9$ amu, $m_H = 1$ amu, $m_N = 14$ amu, and $m_{Be} = 9$ amu).

In the inset of Fig. 4, the phonon dispersion $\omega(q)$ is shown in the frequency interval from 0 to 100 $cm^{-1}$. As can be seen, there are three spectral branches corresponding to acoustic phonons. The acoustic branches tend to zero as they approach the center of the Brillouin zone ($\omega > 0$ at $q > 0$). The absence of imaginary modes testifies to the dynamic stability of the examined crystal. The anisotropy of the acoustic branches is associated with the general anisotropy of the material, which is consistent with the studies of its other physical properties [24, 25].

The density of vibrational states in the crystal is obtained by integrating over all $3N$ vibrational modes ($N$ is the number of atoms in the cell) over the first Brillouin zone. The partial phonon density of states is obtained as the contributions of individual atoms, $i$, to the vibrational spectrum,

$$N_i(E) = \int \frac{d\mathbf{k}}{4\pi^3} |\mathbf{e}_j(i)|^2 \delta(E - E_n(\mathbf{k})), \qquad (12)$$

where $\mathbf{e}_j$ is the eigenvector associated with the vibrational mode with the energy $E_i$ and normalized to the unit length. The sum of the partial contributions made by the phonon density of states gives the total phonon density of states.

In Fig. 5, the partial phonon density of states (PhPDOS) in the $(NH_4)_2BeF_4$ crystal for the contributions of individual atoms to the vibrational spectrum is shown, which was calculated from first principles. Vibrational states corresponding to high-frequency spectral modes at frequencies from 2926 to 3218 $cm^{-1}$, from 1407 to 1550 $cm^{-1}$, and from 1675 to 1751 $cm^{-1}$ correspond to vibrations of light $NH_4$ complexes. Minor contributions are present at low frequencies ($0 \div 250$ $cm^{-1}$) from the vibrational states of nitrogen atoms and near $\omega = 500$ $cm^{-1}$ from hydrogen states. Phonon states in the frequency interval from 741 to 817 $cm^{-1}$ are formed by beryllium vibrations. Low-frequency vibrations in the intervals from 0 to 318 $cm^{-1}$, from 339 to 420 $cm^{-1}$, and from 477 to 590 $cm^{-1}$ are mostly formed by vibrations of fluorine atoms in the $BeF_4$ complexes. Minor contributions of hydrogen and nitrogen states in the low-

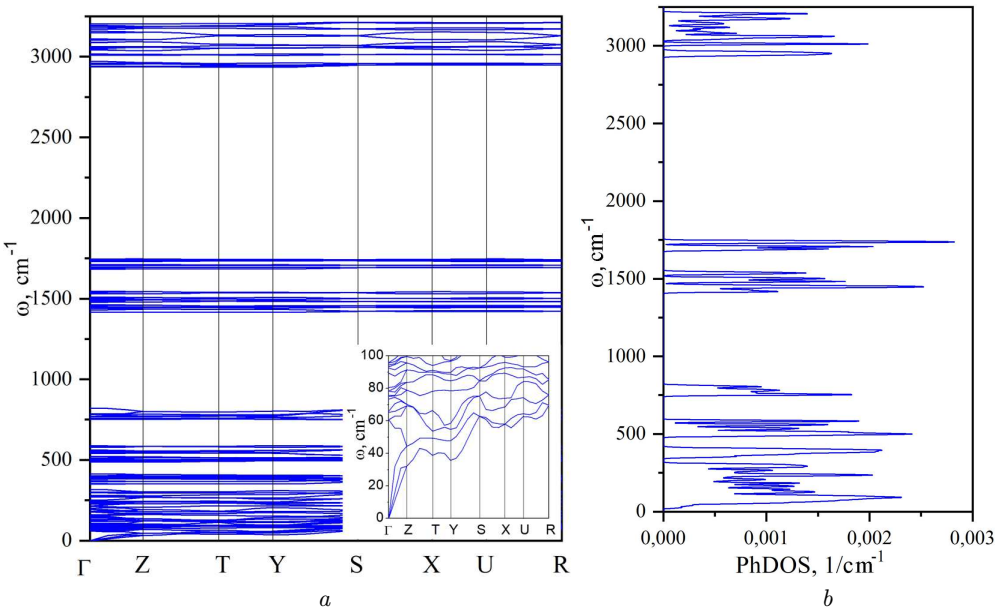


***Fig. 4.*** Phonon dispersion $\omega(q)$ ($a$) and the density of phonon states in the $(NH_4)_2BeF_4$ crystal calculated using the GGA-PBE functional ($b$)

frequency region (<500 $cm^{-1}$) are associated with the interaction (ionic by character) of the corresponding atoms in the $NH_4^+$ complexes with the $BeF_4^{2-}$ groups.

Figure 6 illustrates vibrations of the crystal lattice structure in the $(NH_4)_2BeF_4$ crystal and demonstrates the vectors of atomic vibrations in the lattice. The green arrows mark the directions of atomic motions in the structure during the vibration, and their lengths are proportional to the magnitude of the corresponding displacements from the equilibrium positions. The figure contains seven structures (labeled from $a$ to $g$), which reflect seven types of vibration modes: $A_g$, $B_{1u}$, $B_{2u}$, $B_{3u}$, $B_{3g}$, $B_{1g}$, and $B_{2g}$. The frequency of the corresponding vibration is indicated under each panel.

Due to the large number of vibration modes (180 spectral frequencies), we do not provide a table of vibration frequencies in this article.

### *3.4. Infrared and Raman spectra of the $(NH_4)_2BeF_4$ crystal*

First-principle calculations were used to obtain the infrared and Raman spectra of the crystal under study. In Fig. 7, the calculated spectrum of combined light scattering by the $(NH_4)_2BeF_4$ crystal in the paraelectric phase is shown. The calculations were performed for the excitation wavelength $\lambda_{exc} = 514$ nm and the

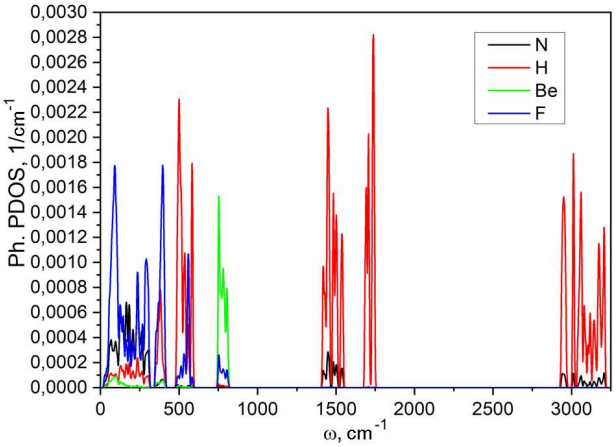


***Fig. 5.*** Partial density of phonon states in the $(NH_4)_2BeF_4$ crystal in the paraelectric phase

temperature $T = 290$ K. The Lorentz broadening was also used to describe the broadening of the spectral lines. According to the group-theoretical analysis, the number of bands in the Raman spectrum should be equal to 69. In practice, the obtained spectrum contains the predicted number of bands, but a substantial part of them has a weak intensity.

The most intense in the Raman scattering spectra is the band at $\omega = 3045$ $cm^{-1}$, which corresponds to the $A_g$-mode of completely symmetric vi-

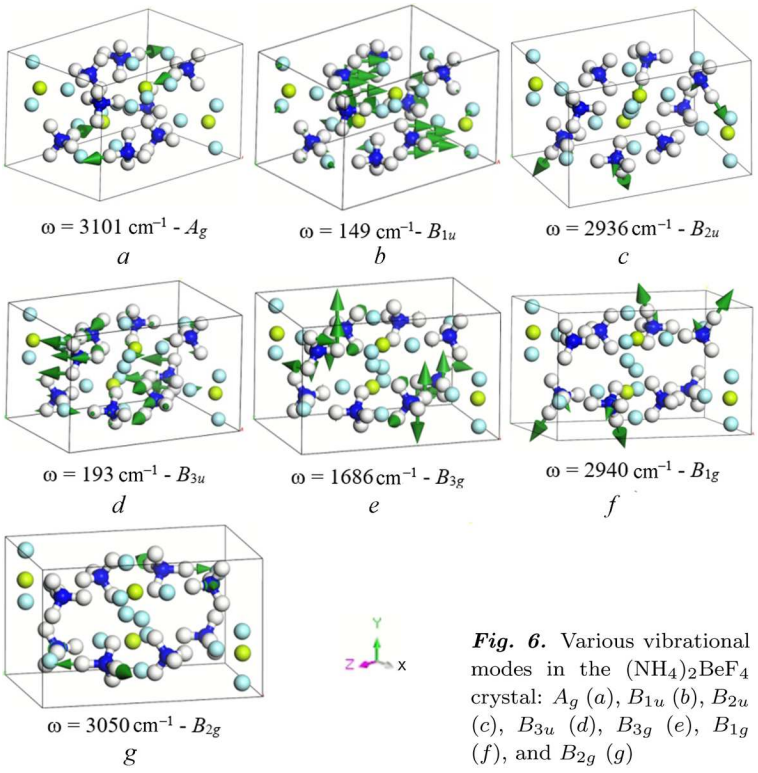


***Fig. 6.*** Various vibrational modes in the $(NH_4)_2BeF_4$ crystal: $A_g$ $(a)$, $B_{1u}$ $(b)$, $B_{2u}$ $(c)$, $B_{3u}$ $(d)$, $B_{3g}$ $(e)$, $B_{1g}$ $(f)$, and $B_{2g}$ $(g)$

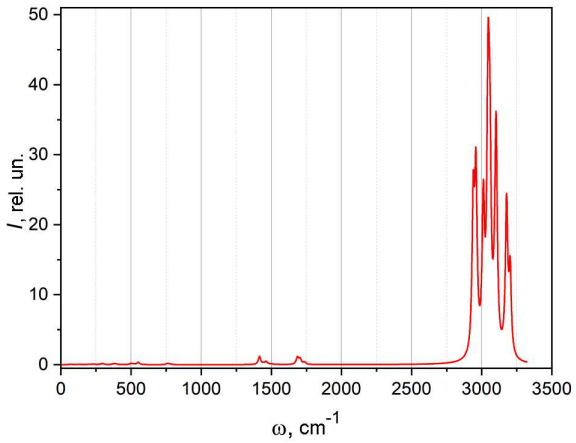


***Fig. 6.*** Raman spectra of the $(NH_4)_2BeF_4$ crystal calculated using the GGA-PBE functional

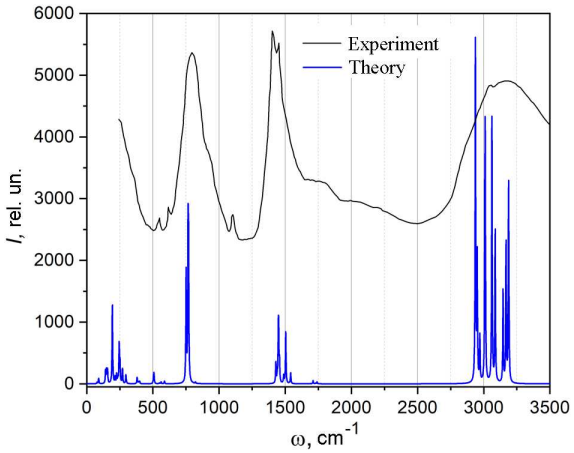


***Fig. 7.*** Infrared spectra of the $(NH_4)_2BeF_4$ crystal calculated using the GGA-PBE functional and experimental spectra obtained in work [1]

bration. This band is formed by the symmetric vibration of the cationic complex $NH_4^+$. Of significant intensities are also the bands in the frequency interval from 2910 to 3220 $cm^{-1}$. The vibrational bands with lower frequencies in the Raman scattering spectrum have much lower intensities.

To our knowledge, only work [7] is devoted to the study of the Raman scattering spectra of the $(NH_4)_2BeF_4$ crystal. In this work, one band in a spectral interval of 0–200 $cm^{-1}$ was obtained at high temperatures. The experimental spectrum contains a wide band from approximately 60 to 80 $cm^{-1}$. At

the same time, the theoretically calculated frequencies corresponding to the active ones in the Raman scattering spectrum are as follows: 60.72 $cm^{-1}$ ($A_g$), 65.29 $cm^{-1}$ ($B_{3g}$), 73.38 $cm^{-1}$ ($A_g$), 75.04 $cm^{-1}$ ($B_{1g}$), and 75.72 $cm^{-1}$ ($B_{3g}$). These frequencies are consistent with the position of the band in the experimental spectrum. Raman scattering spectra of the $(NH_4)_2BeF_4$ crystal in a wider frequency interval have not been studied by other researchers for today.

In Fig. 8, the infrared spectrum of the $(NH_4)_2BeF_4$ crystal calculated from first principles in the frequency interval from 0 to 3500 $cm^{-1}$ is depicted. As one can see, the highest intensity in the calculated spectrum falls on the spectral interval from 2936 to 3190 $cm^{-1}$. In this spectral region, the most intensive is the band corresponding to the $B_{2u}$-mode located at the frequency $\omega = 2935$ $cm^{-1}$. Near a frequency of 1500 $cm^{-1}$, there is a group of low-intensity peaks, which are mainly formed by the vibrations of $NH_4$ tetrahedra. At the frequencies $\omega = 765$ and 769 $cm^{-1}$, there are two closely located phonon bands corresponding to the vibrational modes of the symmetries $B_{2u}$ and $B_{1u}$, respectively. Their intensities are approximately equal to $0.5I$ for the most intensive spectral bands near 3000 $cm^{-1}$.

From Figs. 7 and 8, one can also see that low-frequency vibrations within an interval from 60 to 300 $cm^{-1}$ mainly correspond to infrared vibrations with the change of the dipole moment. At the same time, in the Raman spectra, intensive vibration bands are mainly available at high frequencies spanning from 2936 to 3190 $cm^{-1}$.

Experimental studies of the infrared spectra of the $(NH_4)_2BeF_4$ crystal were carried out in work [1]. For comparison, together with the theoretical infrared spectrum, Fig. 8 also demonstrates the experimental infrared absorption spectrum obtained by the authors within the frequency interval from 250 to 4000 $cm^{-1}$ and at a temperature of 300 K. As one can see, the experimental spectrum also has a complicated structure, being formed by at least four broad bands containing a set of vibrational modes. The positions of the theoretically calculated vibrational levels coincide well with the positions of the experimental bands obtained in work [1].

It is worth noting that the structure of experimental spectra is more complicated than that of theoretical ones due to the presence of the bands formed by combinations of frequencies, the overtones of the corresponding vibrational complexes $NH_4$ and $BeF_4$, the presence of other bands – for example, those associated with vibrations of the O–H complexes of the molecules of crystallization water [$\omega \approx \approx (3200 \div 3650)$ $cm^{-1}$], and so forth.

## 4. Conclusions

Based on the group-theoretical classification, it has been shown that the vibrational spectrum of the $(NH_4)_2BeF_4$ crystal contains 180 vibrational modes; three of them are acoustic branches, and the other 177 are optical ones. A mechanical representation of the vibrational spectrum of the crystal was obtained, and it was shown that the three acoustic branches correspond to the symmetry modes $B_{1u}$, $B_{2u}$, and $B_{3u}$. A representation for the optical modes in the crystal was calculated, and selection rules for the infrared and Raman spectra are obtained. Vibrational modes that are active in the infrared spectrum are inactive in the Raman spectra. The $A_u$-mode is inactive in the vibrational spectra.

A theoretical study of the phonon spectrum of the $(NH_4)_2BeF_4$ crystal in the paraelectric phase has been carried out using the density functional theory and the density perturbation functional theory. The phonon dispersion was obtained for the point sequence $\Gamma \to Z \to T \to Y \to S \to X \to U \to R$ in the first Brillouin zone. It was shown that the phonon spectrum of the $(NH_4)_2BeF_4$ crystal has a complicated structure. The absence of negative frequencies in the calculated spectrum testifies to the dynamic stability of the crystal structure. It was found that the vibrational spectrum of the $(NH_4)_2BeF_4$ crystal in the paraelectric phase contains 180 vibrational modes, which are consistent with the group-theoretical analysis. From the phonon dispersion dependence and the phonon density of states, it was shown that the maximum vibration frequency in the crystal equals 3202.37 $cm^{-1}$. The density of phonon states reflects the band structure of the vibrational spectrum, which points to the relative isolation of the vibrational modes of the tetrahedral groups $BX_4$ in the crystal. It was shown that the theoretically calculated infrared and Raman spectra are consistent with the experimental data available in the literature.

*The results presented in this work were obtained in the framework of the young scientists' project "New mono-, poly-, nanocrystalline dual-purpose materi-*

*als for batteries, hydrogen storage, sensor technology, and electronics" (state registration No. 0123U100599) supported by the Ministry of Education and Science of Ukraine.*


1. Y.S. Jain. Infrared spectra of $(NH_4)_2BeF_4$. *Proc. Indian Acad. Sci.* **87**, 45 (1978).
2. T. Hikita, T. Tsukahara, T. Ikeda. Ultrasonic study of ferroelectric $(NH_4)_2BeF_4$ under hydrostatic high pressure. *J. Phys. Soc. Jpn.* **51**, 2900 (1982).
3. R.C. Srivastava, W.T. Klooster, T.F. Koetzle. Neutron structures of ammonium tetrafluoroberyllate. *Acta Cryst. B* **55**, 17 (1999).
4. G.A. Smolenski. *Physica of Ferroelectric Phenomenons* (Science, 1985) [in Russian].
5. A. Garg, R.C. Srivastava. Ammonium tetrafluoroberyllate(II). *Acta Cryst. B* **35**, 1429 (1979).
6. M. Iizumi, K. Gesi. Incommensurate phase in $(ND_4)_2BeF_4$. *Solid State Commun.* **22**, 37 (1977).
7. M. Wada, A. Sawada, Y. Ishibashi, Y. Takagi. Raman spectra of $(NH_4)_2BeF_4$. *J. Phys. Soc. Jpn.* **43**, 950 (1977).
8. M.D. Segall, P.J.D. Lindan, M.J. Probert, C.J. Pickard, P.J. Hasnip, S.J. Clark, M.C. Payne. First-principles simulation: ideas, illustrations and the CASTEP code. *J. Phys.: Condens. Matter* **14**, 2717 (2002).
9. S.J. Clark, M.D. Segall, C.J. Pickard, P.J. Hasnip, M.I.J. Probert, K. Refson, M.C. Payne. First principles methods using CASTEP, *Z. Kristallogr.* **220**, 567 (2005).
10. W. Korner, C. Elsasser. First-principles density functional study of dopant elements at grain boundaries in ZnO. *Phys. Rev. B* **81**, 085324 (2010).
11. W. Kohn, L.J. Sham. Self-consistent equations including exchange and correlation effects. *Phys. Rev.* **140**, A1133 (1965).
12. J.G. Lee. *Computational Materials Science: An Introduction* (CRC Press, 2012).
13. D.R. Hamann, M. Schluter, C. Chiang. Norm-conserving pseudopotentials. *Phys. Rev. Lett.* **43**, 1494 (1979).
14. H.J. Monkhorst, J.D. Pack. Special points for Brillouin-zone integrations. *Phys. Rev. B* **13**, 5188 (1976).
15. K. Refson, P.R. Tulip, S.J. Clark. Variational density-functional perturbation theory for dielectrics and lattice dynamics. *Phys. Rev. B* **73**, 155114 (2006).
16. B.G. Pfrommer, M. Cote, S.G. Louie, M.L. Cohen. Relaxation of crystals with the quasi-Newton method. *J. Comput. Phys.* **131**, 233 (1997).
17. K. Momma, F. Izumi. VESTA 3 for three-dimensional visualization of crystal, volumetric and morphology data. *J. Appl. Crystallogr.* **44**, 1272 (2011).
18. M.Ya. Rudysh. Electronic structure, optical and elastic properties of $AgAlS_2$ crystal under hydrostatic pressure. *Mater. Sci. Semicond. Process.* **148**, 106814 (2022).
19. M.Ya. Rudysh, A.O. Fedorchuk, M.G. Brik, J. Grechenkov, D. Bocharov, S. Piskunov, A. Popov, M. Piasecki, Electronic, optical, and vibrational properties of an $AgAlS_2$ crystal in a high-pressure phase. *Materials* **16**, 7017 (2023).
20. A.V. Franiv, A.I. Kashuba, O.V. Bovgyra, O.V. Futey. Elastic properties of substitutional solid solutions $In_xTl_{1-x}I$ and sound wave velocities in them. *Ukr. J. Phys.* **62**, 679. (2017).
21. M.S. Dresselhaus, G. Dresselhaus, A. Jorio. *Group Theory: Application To The Physics Of Condensed Matter* (Springer Science and Business Media, 2007).
22. M.Ya. Rudysh, A.I. Kashuba, V.Yo. Stadnyk, R.S. Brezvin, P.A. Shchepanskyi, V.M. Gaba, Z.O. Kohut. Raman scattering spectra of $\beta$-$LiNH_4SO_4$ crystals. *J. Appl. Spectrosc.* **85**, 1022 (2019).
23. M.Ya. Rudysh, M. Piasecki, G.L. Myronchuk, P.A. Shchepanskyi, V.Yo. Stadnyk, O.R. Onufriv, M.G. Brik. $AgGaTe_2$ – the thermoelectric and solar cell material: Structure, electronic, optical, elastic and vibrational features. *Infrared Phys. Technol.* **111**, 103476 (2020).
24. M.G. Brik, I.V. Kityk. Spectroscopic and crystal field studies of $(NH_4)_2BeF_4:Co^{2+}$. *Solid State Commun.* **143**, 326 (2007).
25. N.J.M. Le Masson, Z. Czapla, A.J.J. Bos, J.C. Brouwer, C.W.E. van Eijk. Luminescence and OSL study of the inorganic compounds $Tl^+$-doped $(NH_4)_2BeF_4$ and $(NH_4)_2SiF_6$. *Radiat. Measur.* **38**, 549 (2004).


Received 01.11.24.
Translated from Ukrainian by O.I. Voitenko

*М.Я. Рудиш, М. Пясецький,*
*А.І. Кашуба, Р.С. Брезвін*

КОЛИВНІ СПЕКТРИ КРИСТАЛА $(NH_4)_2BeF_4$ У ПАРАЕЛЕКТРИЧНІЙ ФАЗІ

Досліджено коливні спектри кристала $(NH_4)_2BeF_4$ в параелектричній фазі (просторова група симетрії №62). У рамках теоретико-групового аналізу здійснено класифікацію симетрії коливань в кристалі. Виходячи із перших принципів, в рамках теорії функціонала густини та теорії збурення функціонала густини проведено розрахунки дисперсії фононів та частот коливного спектра кристала $(NH_4)_2BeF_4$. Для цього використано узагальнене градієнтне наближення для опису обмінно-кореляційної взаємодії електронів. Виявлено, що в коливному спектрі кристала присутні 180 коливних мод. Розраховано інфрачервоні спектри та спектри комбінаційного розсіювання кристала $(NH_4)_2BeF_4$ і порівняно їх з експериментальними спектрами.

*Ключові слова*: фонон, фторберилат амонію, DFPT, теорія груп, інфрачервоні спектри, спектри комбінаційного розсіювання, густина фононних станів.